Research Article: Open Access

VIBGYOR ePress

International Journal of
Metallurgy and Metal Physics

ISSN: 2631-5076

Autothermal CO_2 Reforming with Methane Over Crystalline $LaMn_{1-X}Ni_XO_3$ Perovskite Catalysts

Annabathini Geetha Bhavani[1,2*] and Jae Sung Lee[3]

[1]Department of Chemistry, Noida International University Research Innovation Centre, Noida International University, India

[2]Department of Chemical Engineering, Pohang University of Science and Technology (POSTECH), Republic of Korea

[3]School of Nano-Bioscience and Chemical Engineering, Republic of Korea

Abstract

$LaMn_{1-X}Ni_XO_3$ (x = 0.1-0.9) perovskite was prepared by sol-gel method in a single step. All the perovskite catalysts stability was tested over oxy thermal reforming CH_4 with CO_2 for long time-130 h on stream. The $LaMn_{1-X}Ni_XO_3$ perovskite catalyst shows promising catalytical activity for syngas (H_2, CO) production from autothermal reforming. XRD analysis confirms all perovskite catalysts are in single phase and crystalline. Catalysts physiochemical properties were tested by BET analysis for surface area, metallic surface area by CO chemisorption, coke content of spent catalyst by TGA analysis. Catalytic activity was compared in-terms of degree of Ni substitution in lanthanum manganite lattice. The optimal level of Ni substitution in perovskite structure increases surface area, pores volume and metallic surface area, which leads highly stable, active for long time on stream with negligible amounts of coke formation.

Keywords

$LaMn_{1-X}Ni_XO_3$, Ni substitution, Oxygen mobility, Autothermal CH_4 reforming with CO_2

Highlights

- Ni substituted lanthanum manganite $LaMn_{1-X}Ni_XO_3$ (x = 0.1-0.9) is in single phase perovskite structure, confirmed by XRD.
- Catalysts were tested extreme long run of 130 h on stream for oxy thermal reforming of CO_2 with CH_4.
- The high surface area and metal dispersion of catalysts shows tremendous stability and activity in syngas production.
- Rate of reducibility of the catalyst improved the surface oxygen, which helps to trigger deactivation of the catalysts.

Introduction

The process of converting two greenhouse gases (CH_4 with CO_2) to valuables synthesis gas (syngas), a mixture of CO and H_2 by catalytic oxy thermal reforming of methane with carbon dioxide has received significant attention in recent years [1]. Reforming process is generalized by partial oxidation of methane (exothermic reaction), carbon dioxide reforming (endothermic reaction) and oxy thermal reforming of methane with CO_2 (combined exothermic and endothermic reaction). The oxy thermal reforming catalytic process was designed to be economic as it saves energy, because the thermal energy required is generated in the partial oxidation of methane

***Corresponding author:** *Annabathini Geetha Bhavani, Department of Chemistry, Noida International University Research Innovation Centre, Noida International University, Gautama Buddha Nagar, Greater Noida-2013086, India; Department of Chemical Engineering, Pohang University of Science and Technology (POSTECH), San 31, Hyoja-Dong, Pohang 790-784, Republic of Korea, E-mail: geetha.bhavani@niu.edu.in; gitabhavani_19@yahoo.co.in*

Received: December 5, 2017: **Accepted:** January 18, 2018: **Published:** January 20, 2018

Citation: Bhavani AG, Lee JS (2018) Autothermal CO_2 Reforming with Methane Over Crystalline $LaMn_{1-X}Ni_XO_3$ Perovskite Catalysts. Int J Metall Met Phys 3:010

[2]. Oxy thermal reforming reaction has been chosen as a safe and economic way for synthesis gas production in a large-scale.

Perovskite-type mixed oxides (ABO_3), are promising material for catalytic applications involving high temperatures reactions, because of their thermochemical stability and tuneable catalytic performance as oxy thermal reforming reaction requires high temperatures. The perovskite materials are reactivity is couturier by mutable substitution of A- and/or B-site cations. B site elements are partially reduced to form nano-sized metal particles, which are highly active for oxy thermal reforming reaction and resilient to carbon deposition [3,4]. Ni is successfully substituted in $LaFeO_3$ lattice, and reduced to nanoparticles to improve the reactivity and stability without collapsing the $LaFeO_3$ perovskite structure. The $LaNiO_3$ perovskite catalyst in reforming of CH_4 with CO_2 exploration reviles, metallic Ni for activating CH_4 and basic La_2O_3 for CO_2 reforming [5].

Noble metal based catalysts (Pt and Ru) are well practiced for oxy thermal reforming reaction for a high activity with no carbon deposition [6] with a drawback of cost of the metals. The non-noble metal based catalysts (like Fe, Ni, Co, Mn) are practiced of their appreciable catalytic activity, good stability and low price with a drawback of metal sintering [7]. Ni-based perovskite in the form of $BaZr_{(1-x)}Me_xO_3$ was evaluated and the results were compared the synthesis methods of sol-gel method and auto-combustion method and sol-gel found to be promising route for the use of Ni in this process with good activity can be achieved from temperature of 973 K [8]. Syngas production by CO_2 reforming of methane on $LaNi_xAl_{1-x}O_3$ perovskite catalysts prepared by sol-gel method with prominent bench mark results [9]. Nickel-based catalyst by impregnation and perovksites by sol gel (SG) and co precipitation (CP) method for CO_2 reforming of CH_4 Conversion of CH_4 and CO_2 were found in the order: $LaNiO_3$(CP) > 10% Ni/ZrO_2-Al_2O_3 > $LaNiO_3$(SG) > 10% Ni/K_2O-Al_2O_3 > 10% Ni/MgO-Al_2O_3 > $LaCoO_3$(CP) > $LaCoO_3$(SG) > 10% Ni/CeO_2-Al_2O_3 > 10% Ni/-Al_2O_3 > 5% Ni/-Al_2O_3 > 20% Ni/-Al_2O_3. $LaNiO_3$ (CP) gave high activity and stability due to further reduction of B-site cations which remain distributed in the structure and form well dispersed and stable metal particle catalysts which improved the stability and activity [10].

The present work to synthesize the highly crystalline porous metal catalysts and examined the activity of Mn and Ni loadings on physico-chemical properties. We aimed to develop coke resistance $LaMn_{1-X}Ni_XO_3$ perovskite catalysts to strong activity and stable production of syngas (H_2 and CO). By varying Ni and Mn factions like x = 0.1, 0.3, 0.5, 0.7, 0.9 respectively, by sol-gel method in order to improve its activity for oxy thermal reforming of methane and to find optimum value of bimetallic synergy.

Experimental

Catalyst preparation and characterization

$LaMn_{1-x}Ni_XO_3$ (x = 0.1, 0.3, 0.5, 0.7, 0.9) perovskite catalysts are synthesized by sol-gel method. The stoichiometric amounts of lanthanum $La(NO_3)_3{\cdot}4H_2O$, manganese $Mn(NO_3)_2{\cdot}4H_2O$ and nickel nitrates $Ni(NO_3)_2$ are used as precursors. Citric acid and total metal ions of 1:1.5 of molar ratio was adopted to obtain the perovskite oxides materials. The various forms of polycondensation (sol) reactions to form diphasic system containing both a liquid phase and solid phase (gel). Primary powder formed by firing resulted gel at 350 °C for 5 h. After reaching to room temperature again thermally treated at 850 °C for 5 h.

The analysis of perovskite crystal phases was performed using powder X-ray diffraction (XRD) technique. The texture of the samples was characterized by the BET N_2 adsorption-desorption method at -196 °C using Micromeritics 2010 sorptometer. The BJH method was applied for determination of pore size distribution. Relative elemental composition of the prepared perovskite catalysts are analysis by atomic adsorption spectroscopy. AutoChem program in CO pulse chemisorptions analysis was used to account the metal dispersion (%) and metallic surface area (m^2/g) of thermally treated catalysts. XPS analysis was used to quantify O 1s core level spectra. Spent catalysts are analyzed by thermogravimeter (Mettler Toledo, TG-SDTA 851 instrument). All the analysis procedures are detailed in our earlier report [7,11].

Catalytic test procedure

Tubular fixed-bed flow reactor was used for catalytic tests at atmospheric pressure. 100 mg of catalyst was preheat at 500 °C for 30 min, for reduction treatment under H_2 at 500 °C for 2 h. The mole ratio of CH_4:CO_2:O_2-1:0.8:0.2 reactant gases are fed into the reactor at gas hourly space velocity (GHSV)-243,000 h^{-1} and gas flow rates are controlled by mass flow meters at 800 °C. After 30 min of steady-state operation of the reaction the conversion and selectivity were determined. The product mixtures were analyzed by online gas chromatograph and the calculation of products analysis shown in our earlier report [7].

Result and Discussions

BET and x-ray diffraction

Surface properties of catalysts enumerated in Table 1. All the catalyst shows comparable surface areas and compare to all the catalyst $LaMn_{0.3}Ni_{0.7}O_3$ catalyst shows high surface area of 9.573 m^2/g and the $LaMn_{0.9}Ni_{0.1}O_3$ catalyst shows lowest 1.246 m^2/g. These results clearly indicate that

Table 1: Surface area and elemental composition of $LaMn_{1-x}Ni_xO_3$ (x = 0.1, 0.3, 0.5, 0.7, 0.9) perovskite catalysts.

Catalyst[a]	Ni ratio	Surface area m^2/g	Average pore diameter (Å)	Relative elemental composition		
				La	Mn	Ni
$LaMn_{0.9}Ni_{0.1}O_3$	x = 0.1	1.246	3.01	99.01	0.9	0.09
$LaMn_{0.7}Ni_{0.3}O_3$	x = 0.3	2.737	4.74	99.01	0.8	0.19
$LaMn_{0.5}Ni_{0.5}O_3$	x = 0.5	4.291	9.14	99.03	0.49	0.48
$LaMn_{0.3}Ni_{0.7}O_3$	x = 0.7	9.573	13.52	99.00	0.3	0.7
$LaMn_{0.1}Ni_{0.9}O_3$	x = 0.9	1.089	2.86	99.01	0.1	0.89

[a]Prepared by Sol-Gel method.

Table 2: Chemisorption properties of $LaMn_{1-x}Ni_xO_3$ (x = 0.1, 0.3, 0.5, 0.7, 0.9) perovskite catalysts.

Catalyst	Metal dispersion (%)[b]	Metallic surface area (m^2/g)[b]	Coke content (wt.%)[c]
$LaMn_{0.9}Ni_{0.1}O_3$	0.4	0.7	8.68
$LaMn_{0.7}Ni_{0.3}O_3$	1.01	0.6	9.18
$LaMn_{0.5}Ni_{0.5}O_3$	2.4	1.3	7.30
$LaMn_{0.3}Ni_{0.7}O_3$	3.9	2.5	0.94
$LaMn_{0.1}Ni_{0.9}O_3$	0.3	0.4	14.91

[b]Measured from AutoChem program in CO pulse chemisorptions; [c]Coke content is measured after 130 h of oxy thermal reforming of CO_2 with methane by TGA analysis.

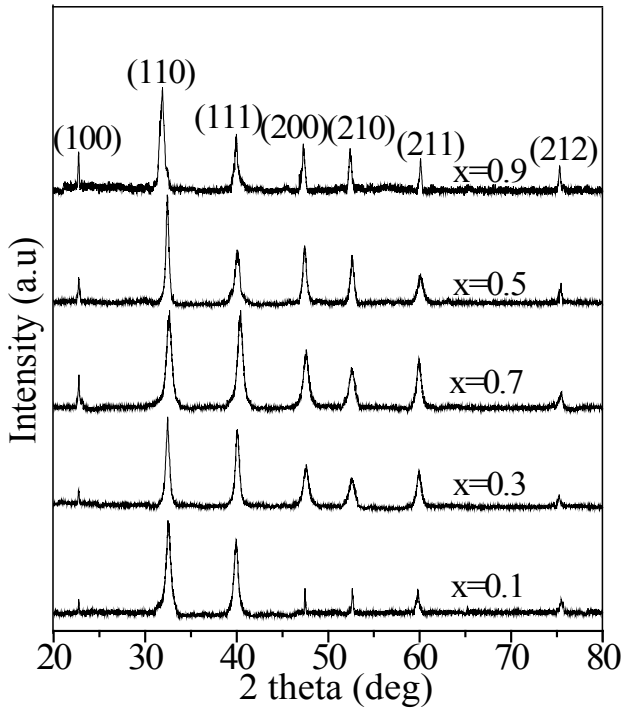

Figure 1: XRD patterns of various $LaMn_{1-x}Ni_xO_3$ metal ratios of catalysts are a) x = 0.7; b) x = 0.9; c) x = 0.5; d) x = 0.3; e) x = 0.1, catalysts after 600 °C of calcination.

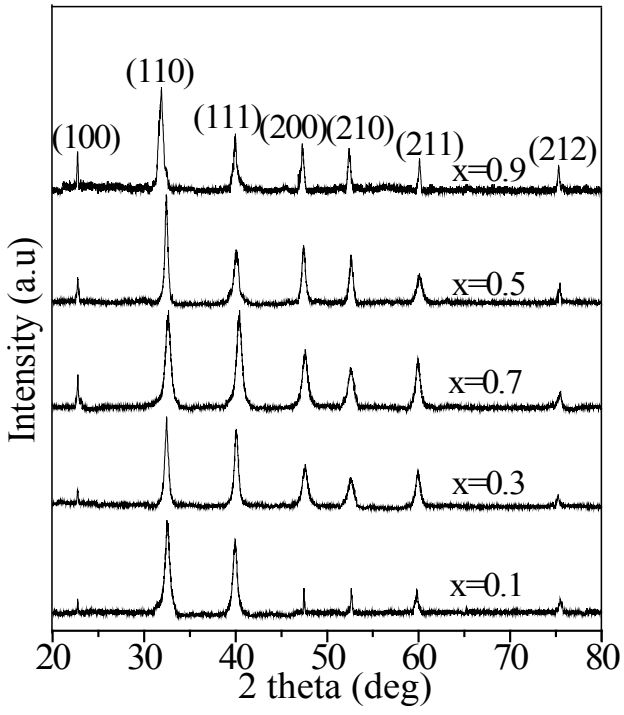

Figure 2: XPS analysis for $LaMn_{1-x}Ni_xO_3$ samples, O 1s core level spectra.

significant Ni substitution in enhancement of surface area as well as pore volume. The perovskite materials of initial sol are well matched with elemental analysis of the prepared.

The calcinied $LaMn_{1-x}Ni_xO_3$ powder XRD patterns are revealed in Figure 1, indicates all the samples are in single perovskite phase with high crystallinity. No impurity phase was found, such as NiO, MnO_3, Mn_2O_3. The catalyst x = 0.7, XRD reflection is intense compare to other x ratios. Furthermore, increasing Ni substitution leads to progressive structural distortion by the lattice enlargement [12].

Photoelectron spectroscopy (XPS)

Table 2 shown the chemisorption measurements of $LaMn_{1-x}Ni_xO_3$ samples to determine the exposed metal surface area with CO as a probe molecule [7]. All catalysts shows significant metallic surface area and dispersion. Equate to all catalysts $LaMn_{0.3}Ni_{0.7}O_3$ shows 3.9 m^2/g of dispersion and 2.5% of highest metallic surface

area and the $LaMn_{0.9}Ni_{0.1}O_3$ catalyst has lowest amount of dispersion of 0.4% and 0.7 m^2/g of metallic surface area. All the series results illustrates the profound influence of the Ni in amount of dispersion and metallic surface area.

Figure 2 states the XPS analysis of O 1s peaks of $LaMn_{1-X}Ni_XO_3$ various metal ratios of reduced catalysts. The binding energy of O 1s revels two distinctive peaks for all the catalysts. The lattice oxygen O^{2-} ($O_{lattice}$) peak is found at low binding energy (BE 530.0 eV) and adsorbed oxygen species ($O_{adsorbed}$) peak found at high binding energy (BE 531.4 eV) [11]. In the present case, proficiently rises the intensity of both lattice oxygen and adsorbed oxygen species by increase in Ni fractions from 0.1 to 0.3 ratios, but a further decreases the intensity of the two peaks by increase to 0.5 and 0.9 ratio. Results clearly indicates the different degrees of oxygen close to the surface due to their different surface areas.

Oxy thermal reforming of methane with CO_2

The key oxy thermal reforming reaction shown equation (1) takes place in a single chamber where partially oxidation of CH_4 (exothermic reaction) and CO_2 reforming (endothermic reaction) takes place. The combination of both reactions is a very significant triumph to obtain temperature compensation of the process. The overall reaction can be described in the following equation:

$$2CH_4 + O_2 + CO_2 \rightarrow 3H_2 + 3CO + H_2O \quad (1)$$

The LMN catalysts were tested for oxy thermal reforming reaction after reduction in an equimolar H_2/N_2 flow at 770 °C for 1 h. Catalytic screening results of methane and CO_2 conversion are shown in Figure 3A and Figure 3B and selectivity of H_2 and CO are shown in Figure 4A and Figure 4B, respectively at 800 °C. The spent catalysts (after 130 h of on-stream reaction) were analysed to quantify the amounts of coke formed were listed in Table 2 by TGA analysis. Catalytic performance of $LaMn_{0.9}Ni_{0.1}O_3$ catalyst is found to be stable activity with CH_4 and CO_2 conversions are around 55% and 48% with 36% of H_2 selectivity and left 6.48% of coke content. Increase in Ni content by 0.5% in $LaMn_{0.5}Ni_{0.5}O_3$ catalyst show highly stable performance compare to $LaMn_{0.7}Ni_{0.3}O_3$. The CH_4 and CO_2 conversions increases

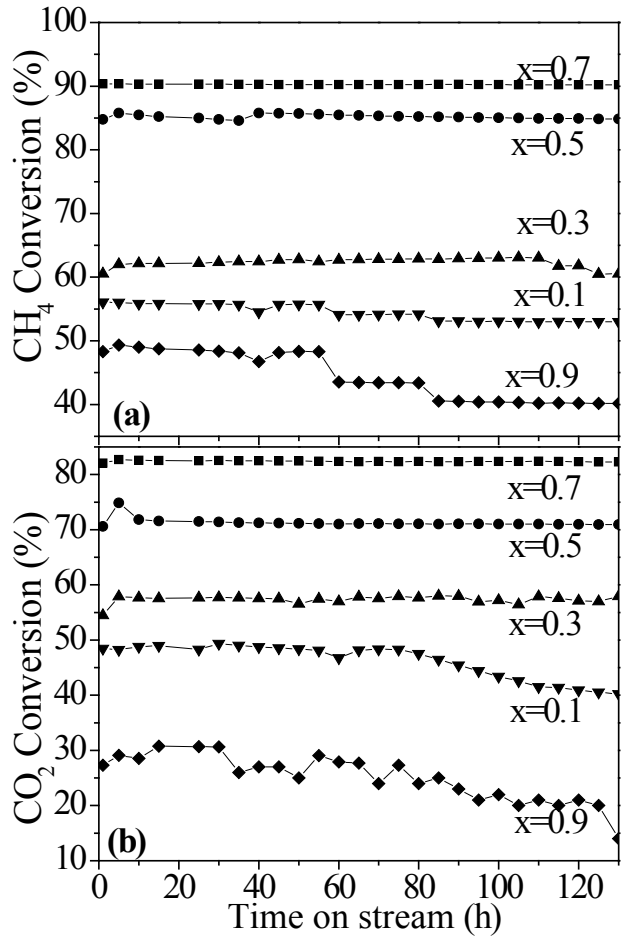

Figure 3 (a-b): CH_4 and CO_2 conversions over various $LaMn_{1-X}Ni_XO_3$ metal ratios at 800 °C a) x = 0.7; b) x = 0.9; c) x = 0.5; d) x = 0.3; e) x = 0.1, at CH_4:CO_2:O_2-1:0.8:0.2 mole ratios.

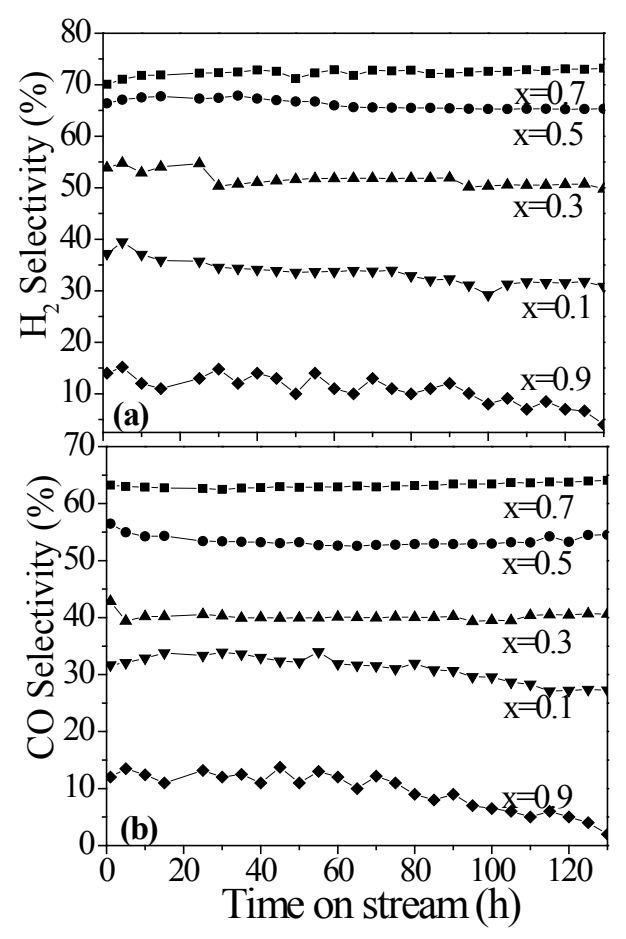

Figure 4 (a-b): Product distribution of H_2 and CO at 800 °C over $LaMn_{1-X}Ni_XO_3$ metal ratios of catalysts are a) x = 0.7; b) x = 0.9; c) x = 0.5; d) x = 0.3; e) x = 0.1, at CH_4:CO_2:O_2-1:0.8:0.2 mole ratios of 800 °C.

from 60% to 84.8% and from 55% to 71%, as well as H_2 and CO selectivities, respectively. $LaMn_{0.5}Ni_{0.5}O_3$ catalyst shows a notable surge in surface area and pore diameter, this reveals that reactants are allow to access pores for conversion and leads high and stable syngas selectivity. $La_{0.9}Ba_{0.1}NiO_3$ and $LaNiO_3$ perovskite catalysts [13] are studied over dry reforming of methane, where CO_2 from 39% to 51% and CH_4 conversion increased from 45% to 55% with threshold addition of Ba. By increasing 0.7% of Ni content in $LaMn_{0.3}Ni_{0.7}O_3$ catalyst reverts incredible stability in performance and without a noticeable deactivation. The dissociation (reforming) of CO_2 releases the adsorbed oxygen that reacts with deposited carbon (formed by partial oxidation of methane) to form CO, thereby coke formation reduces remarkably [14]. Apart from oxygen species released by CO_2, O_2-TPD analysis reveals all the perovskite catalysts shows oxygen species are readily accessible for oxy thermal reforming reaction. Hence, the amounts of surface and lattice oxygen offered on the surface are the robust connection with activity and deactivation of the catalysts. It was clear that critical step is activation of CO_2 releases the oxygen species has to be replenished by reactant molecules to sustain the turnover of the catalytic cycle [13,15].

XRD of $LaMn_{0.1}Ni_{0.9}O_3$ catalyst is found to be low intensity, results unstable activity with CH_4 and CO_2 conversions are around 49% and 28% with 15% of H_2 selectivity and left 14.91% of coke content shown in Table 2, which has high amount of Ni substitution. CO chemisorption results low metallic surface area and dispersion leads to quick deactivation of the catalyst. In our earlier report [7,11] we predicted different pathways of methane decomposition over a reduced metallic site of Ni° and disproportionation of CO mechanism over lattice oxygen adjacent to the metallic site over Ni based trimetallic mixed oxide catalyst as well as Ni loaded lanthanum manganite perovskite catalyst. The similar phenomena observed in present LMN series.

In case of $LaMn_{1-X}Ni_XO_3$ (x = 0.5-0.7) perovskite catalysts shows intense XPS peaks of lattice oxygen that effectively activates and maintains stability of the catalytic cycle. Coke gasification is dynamic role played by the mobility of oxygen species, which comes from bulk to surface. Xiaoping, et al. [16] used active, oxygen donor $LaFeO_3$ perovskite catalyst for partial oxidation of methane to produce synthesis gas. Hence $LaMn_{0.3}Ni_{0.7}O_3$ catalyst results the highest to yield of synthesis gas with a best reforming performance. Oxy thermal reforming reaction also well correlation with percentage of coke formed on different catalysts.

Effect of metallic surface area and dispersion on oxy thermal reforming reaction

The percentage of metallic surface and dispersion of the active metal (Ni) is directly proportional to the catalysts activity and stability especially for long time on stream. The metal surface area and metal dispersion show a good agreement with the measured by CO chemisorption. $LaMn_{0.9}Ni_{0.1}O_3$ catalyst show metallic surface area of 0.7 m^2/g and dispersion of 0.4%. Increasing Ni fractions in $LaMn_{0.7}Ni_{0.3}O_3$ catalyst show improvement in metallic surface area of 1.01 m^2/g and dispersion of 0.6%. Maximum surface area of 3.9 m^2/g and dispersion of 2.5% reflects over $LaMn_{0.3}Ni_{0.7}O_3$ catalyst. Thus, the highest initial activity and stability of $LaMn_{0.3}Ni_{0.7}O_3$ catalyst could be attributed to elevated surface oxygen and well dispersed metallic surface area. The metallic dispersion parameters are summarized in Table 2 are well interrelated to other catalysts activity. It is well interrupted that smaller metal particles give higher dispersion and larger metal surface areas. Further increase in Ni substitution in $LaMn_{0.1}Ni_{0.9}O_3$ catalyst decrease the dispersion may due to bulk formation by over lapping. Our previous report [17] shows dispersed nanosized metallic nickel particles will reflected the significant influence to contributing oxy thermal reforming performance.

The larger Ni particle occupies enough surface area that reduces coke gasification as it needs both metallic area and surface oxygen over support. The larger metal particles leading to tend to form polymerize carbon atoms that accumulate and leads loss of activity stop the catalyst turnover. Thus, bimetallic synergy of Mn and Ni in a threshold percentages boosts the pronounced reducing property of particle sizes, and also depends the nature of the added second metal. The amount of CO_2 chemisorbs (disproportionation) is directly proportional to the surface oxygen and metal dispersion. Threshold values of metals could be the primary factor in changes of physiochemicals properties of the catalyst [17].

Conclusion

Ni was successfully substituted in Over $LaMnO_3$ lattice Ni substituted is by sol-gel process and developed the highly crystalline phase of $LaMn_{1-X}Ni_XO_3$ with chemical homogeneity. The threshold level of Ni substitution leads to high surface area, pores volume and uniformity in metallic particle dispersion. This bimetallic synergy of Ni and Mn perovskite catalyst improved reducibility leads to surface oxygen comes from bulk toward surface. Oxy thermal reforming reactions, decompositions of CH_4 occurs over metallic sites and dissociations of CO_2 occurs over metal associated with adsorbed oxygen leads outstanding syngas selectivity, and forceful maintenance of catalyst surface with little coke formation. In nutshells, supercilious performance of improved $LaMn_{1-X}Ni_XO_3$ catalysts depends on donating lattice oxygen to the catalytic cycle.

References

1. S Diego, L Russo, PL Maffettone, L Salemme, M Simeone,

et al. (2009) Modeling Temperature Profiles of a Catalytic Autothermal Methane Reformer with Nickel Catalyst. Ind Eng Chem Res 48: 1804-1815.

2. S Ayabe, H Omoto, T Utaka, R Kikuchi, K Sasaki, et al. (2003) Catalytic autothermal reforming of methane and propane over supported metal catalysts. Applied Catalysis A: General 241: 261-269.

3. S Royer, H Alamdari, D Duprez, S Kaliaguine (2005) Oxygen storage capacity of $La_{1-x}A'_xBO_3$ perovskites (with A′ = Sr, Ce; B = Co, Mn)-relation with catalytic activity in the CH_4 oxidation reaction. Applied Catalysis B: Environmental 58: 273-288.

4. VM Jimenez, JP Espinos, AR Gonzalez-Elipe (1998) Control of the stoichiometry in the deposition of cobalt oxides on SiO_2. Surface and Interface Analysis 26: 62-71.

5. T Osaki, T Mori (2001) Role of potassium in carbon-free CO_2 reforming of methane on k-promoted Ni/Al_2O_3 catalysts. Journal of Catalysis 204: 89-97.

6. OA Sęyma, E Ozensoy, AE Aksoylu (2009) The effect of impregnation strategy on methane dry reforming activity of Ce promoted Pt/ZrO_2. International Journal of Hydrogen Energy 34: 9711-9722.

7. AG Bhavani, WY Kim, JY Kim, JS Lee (2013) Improved activity and coke resistance by promoters of nanosized trimetallic catalysts for autothermal carbon dioxide reforming of methane. Applied Catalysis A: General 450: 63-72.

8. BD Caprariis, PD Filippis, A Petrullo, M Scarsella (2015) Methane dry reforming over nickel perovsikite catalysts. Chemical Engineering Transactions 43: 991-996.

9. TV Sagar, D Padmakar, N Lingaiah, KS Ramarao, IAK Reddy, et al. (2017) Syngas production by CO_2 reforming of methane on $LaNi_xAl_{1-x}O_3$ perovskite catalysts: influence of method of preparation. J Chem Sci 129: 1787-1794.

10. Sandeep K Chawl, Milka G, Femina Patel, Sanjay Patel (2013) Production of synthesis gas by carbon dioxide reforming of methane over nickel based and perovskite catalysts. Procedia Engineering 51: 461-466.

11. AG Bhavani, WY Kim, JS Lee (2013) Barium substituted lanthanum manganite perovskite for co_2 reforming of methane. ACS Catalysis 3: 1537-1544.

12. GR Moradi, M Rahmanzadeh, S Sharifnia (2010) Kinetic investigation of CO_2 reforming of CH_4 over La-Ni based perovskite. Chemical Engineering Journal 162: 787-791.

13. J Wei, E Iglesia (2004) Isotopic and kinetic assessment of the mechanism of methane reforming and decomposition reactions on supported iridium catalysts. Phys Chem Chem Phys 6: 3754-3759.

14. M Nagabhushana, RPS Chakradhar, KP Ramesh, V Prasad, C Shivakumara, et al. (2008) Magnetoresistance studies on barium doped nanocrystalline manganite. Journal of Alloys and Compounds 450: 364-368.

15. A García, N Becerra, L García, I Ojeda, E López, et al. (2011) Structured perovskite-based oxides: use in the combined methane reforming. Advances in Chemical Engineering and Science 1: 169-175.

16. D Xiaoping, Y Changchun, L Ranjia, W Qiong, S Kaijiao, et al. (2008) Effect of calcination temperature and reaction conditions on methane partial oxidation using lanthanum-based perovskite as oxygen donor. Journal of Rare Earths 26: 341-346.

17. AG Bhavani, WY Kim, JS Lee, JW Lee (2015) Influence of metal particle size on oxidative co_2 reforming of methane over supported nickel catalysts: effects of second-metal addition. Chem Cat Chem 7: 1445-1452.

Citation: Bhavani AG, Lee JS (2018) Autothermal CO_2 Reforming with Methane Over Crystalline $LaMn_{1-x}Ni_xO_3$ Perovskite Catalysts. Int J Metall Met Phys 3:010